

## NEXT GENERATION INLINE MINORITY CARRIER LIFETIME METROLOGY ON MULTICRYSTALLINE SILICON BRICKS FOR PV

N. Schüler<sup>1\*</sup>, D. Mittelstrass<sup>1</sup>, K. Dornich<sup>1</sup>, J.R. Niklas<sup>1</sup> and Holger Neuhaus<sup>2</sup>

<sup>1</sup> Freiberg Instruments GmbH, Am St. Niclas Schacht 13, 09599 Freiberg, Germany

<sup>2</sup> Solar World Innovations GmbH, Berthelsdorfer Str. 111 A, 09599 Freiberg, Germany

### ABSTRACT

In this paper the novel method MDP (microwave detected photoconductivity) [1-4] will be introduced to the field of contact less inline metrology at bricks. By the application of a widely advanced microwave detection technique, it is now possible to map minority carrier lifetime and photoconductivity simultaneously, with a so far unsurpassed combination of spatial resolution, sensitivity, and measurement speed. Beside these two parameters the iron concentration can be detected and analyzing the photoconductivity at steady state in comparison with the minority carrier lifetime, a lot of additional information can be derived. This paper will show first examples of minority carrier lifetime and photoconductivity maps, along with resistivity linescans and iron concentration maps of whole bricks measured inline. Furthermore simulations will be provided. Solving the transport equations for electrons and holes during the measurement at bricks, it can be proven that the measured effective lifetime deviates only lightly from the actual bulk lifetime. Furthermore it becomes clear that a steady state generation is more suited for brick measurements than non-steady state methods.

### INTRODUCTION

Destruction free measurements of minority carrier lifetime like  $\mu$ PCD (microwave detected photoconductivity decay) [5] and QSSPC (quasi steady state photo conductance) [6] are well established and widely used for process control and characterization of defects in crystalline silicon. Since the minority carrier lifetime is very sensitive to all sorts of electrically active defects and therefore the material quality, it is a useful parameter for classifying wafers.

In a former paper, the method MDP was presented as a new method for inline wafer measurements [3]. A full wafer map with a spatial resolution of 2.8 mm can be obtained in less than 0.7 seconds. As it was shown in [3], it is possible to differentiate between good and very bad wafers for example in the top and bottom of the brick, even at as-grown wafers.

To enhance the yield of high quality solar cells, inline brick measurements even allow sorting out low quality parts before the sawing of wafers.

MDP enables the measurement of minority carrier lifetime and photoconductivity maps along with resistivity linescans of two surfaces of a brick during production with a resolution of 1mm in about 2 min. By measuring adjacent

columns even a 3d-picture of the whole block can be constructed. The photoconductivity is closely related to the resistivity, minority carrier diffusion length and mobility. With the ability to measure the spatial resolved photoconductivity a new potential possibility of detecting pn-changes in the brick arises, hence more exact criteria for cutting off bad parts of the brick can be found. A further feature is the determination of the iron concentration.

In the following chapters measurements and simulations will show that, since MDP uses a steady state photogeneration, the measured lifetime is dominated by the bulk lifetime instead of the surface, enabling e.g. the iron determination.

The comprehensive software developed for the MDP measuring systems provides a lot of useful features, such as suggesting the cut off parts of the brick, indicating pn-changes or providing different averaging methods for the lifetime.

### SIMULATIONS

In order to correctly interpret lifetime measurements at thick samples the carrier profile that develops during the measurement has to be simulated. It is necessary to simulate the carrier density as a function of time and space as correctly as possible. This is achieved with a partial differential equation system, which is directly derived from the carrier transport equations. The equation system includes carrier diffusion, drift current, generation and recombination.

The dominant recombination center was assumed to be FeB with a concentration of  $10^{12} \text{ cm}^{-3}$  [7].

From the gained simulated carrier profiles a sensor-weighted average carrier density for every determined time can be evaluated as follows [8]:

$$\Delta n_{\text{sensor}} = \frac{\int_0^w \Delta n(x) \cdot w(x) dx}{\int_0^w w(x) dx} \quad (1)$$

$$\text{with } w(x) = e^{-\frac{x}{\delta}}, \text{ and } \delta = \sqrt{\frac{\rho}{\pi \nu \mu_0 \mu_r}} \quad (2)$$

where  $\delta$  is the skin depth of the microwave,  $\nu$  the frequency of the microwave and  $\mu_0$  and  $\mu_r$  are the permeability of vacuum and the sample respectively. From the transient of this sensor-weighted carrier density the effective lifetime can be extracted, which should agree closely to the measured lifetimes.

### METHOD

Similar to the widely used method  $\mu$ PCD, MDP measures the time dependent photoconductivity during and after the excitation of a sample with a rectangular light pulse. But other than  $\mu$ PCD this is achieved by measuring the *absorption* of a microwave with a resonant microwave cavity and not only by measuring the reflection. Hence the detection sensitivity of MDP is very high and enables the application also of weak laser pulses with unlimited duration. Thus experiments also with a steady state photo generation regime (200  $\mu$ s, 500 mW) or with  $\mu$ PCD conditions (200 ns light pulse; 16 W) are facilitated. A unique feature giving MDP the flexibility needed to adjust to different demands.

For all measurements conducted at bricks a steady state photogeneration is used, since this lead to measured lifetimes that better resemble the bulk properties. All measurements presented in this paper were performed inline, within 2 min and a 1 mm resolution. In table 1 the measurement conditions are summarized.

**Table1 Measurement conditions**

	MDP
excited area	0.79 mm <sup>2</sup>
pulse width	200 $\mu$ s
photons/pulse	4.9x10 <sup>14</sup>
laser power [mW]	500
photons/(pulse cm <sup>2</sup> )	6.3x10 <sup>16</sup>

### RESULTS

Inline brick measurements allow to investigate the crystal quality as early as possible in the production process. Impurities in the cast material or effects of the growth process can be recognized directly after growing and sawing the bricks. Besides a full electrical characterization of two surfaces of each brick, even Fe concentration measurements are possible. Along with the minority carrier lifetime, the photoconductivity at steady state and the resistivity is measured. Furthermore the photoconductivity allows to gain information about pn junctions in the brick. With these measurements of two surfaces of each brick, even a 3d model of each block can be obtained and furnace properties can be optimized. Some examples of possible applications are given in the next chapters.

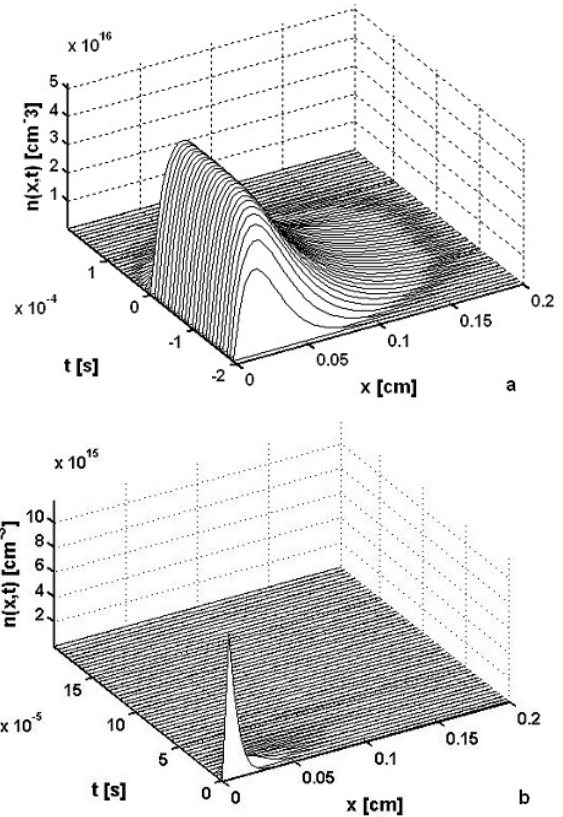


**Figure 1 Carrier profile in a 2 mm thick sample with  $N_{dot} = 10^{16} \text{ cm}^{-3}$  at 300 K for a typical MDP (a) defined by light pulse duration of 200  $\mu$ s,  $\lambda = 978 \text{ nm}$ , microwave frequency  $\nu = 9.4 \text{ GHz}$  and a  $\mu$ PCD (b) measurement defined by light pulse duration of 200 ns,  $\lambda = 904 \text{ nm}$ ,  $\nu = 10.4 \text{ GHz}$ , for both cases FeB was used as the recombination center [9]**

### Inline brick measurements

If thick samples with as-grown surfaces are measured, the skin depth of the measurement microwave and the developing carrier profile has to be taken into account. Both parameters have a huge influence on the measured effective lifetime. The recombination at the surface influences the measurement result to a different extent, if for example a short pulse (e.g.  $\mu$ PCD) or steady state photogeneration (e.g. MDP and QSSPC) is used. In an earlier publication the influence of different measurement regimes along with different laser wavelengths or doping concentrations on the measured lifetime was studied extensively by simulating the carrier profiles [9]. The results can be summarized as follows: an effective lifetime that is only lightly influenced by the surface can be obtained if a steady state photogeneration, a laser wavelength near 1100 nm and a small doping concentration is used. The difference between short pulse and steady state is mainly due to the diffusion of the carriers, if  $\mu$ PCD and MDP are considered, since both methods use similar microwave frequencies. If

a short pulse photogeneration is used the penetration depth of the carrier profile equals the penetration depth of the laser wavelength ( $d$  (980 nm) = 100  $\mu\text{m}$ ), because the carriers cannot diffuse during the light pulse. Contrary to that, the penetration depth of the carrier profile of a steady state photo generation equals the penetration depth of the laser wavelength plus the diffusion length of the carriers. Figure 1 displays the simulated carrier profiles for a typical MDP and  $\mu\text{PCD}$  measurement.

The consequence is that the lifetime measured by steady state methods is more suited to investigate the bulk properties of a thick sample. Hence e.g. the cutting criteria determined by these measurements are more realistic and the determination of the iron concentration is enabled.

### Iron detection

As mentioned above the effective lifetime measured by MDP is not strongly influenced by the surface of the brick. Hence an iron detection, where the lifetime deviation before and after the dissociation of FeB pairs is used, is possible. For this the following equation is used:

$$[Fe] = C_{\Delta n, N_{dot}} \cdot \left( \frac{1}{\tau_{Fe_i}} - \frac{1}{\tau_{FeB}} \right) \quad (3)$$

By simulating the carrier profiles of a typical steady state and short pulse photogeneration the effect of FeB dissociation on the measured lifetime by these two methods can be determined. The deviation  $\Delta\tau$  of the effective lifetime before and after the dissociation versus the iron concentration for the two different measurement regimes is displayed in figure 2. The same parameters as in figure 1 were used for the simulation.

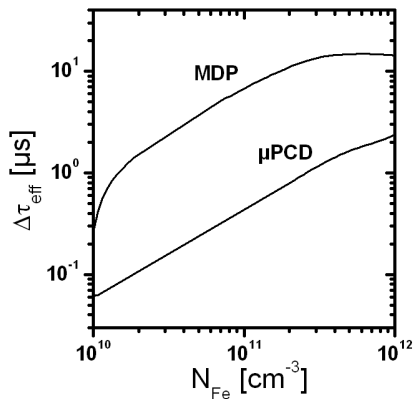
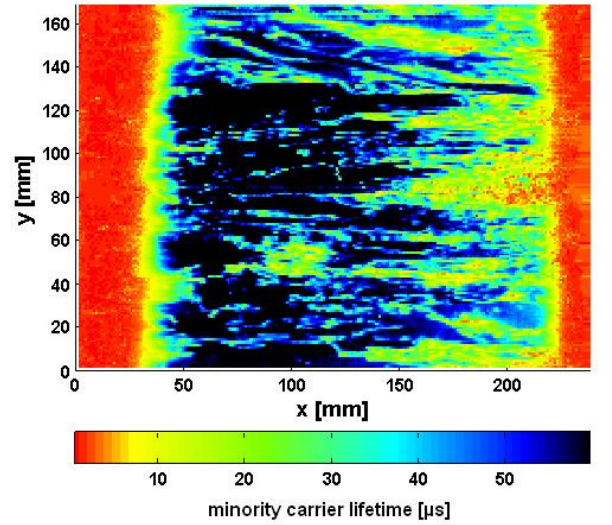


**Figure 2** Deviation in the effective lifetime before and after the FeB dissociation versus Fe density for a typical MDP and  $\mu\text{PCD}$  measurement

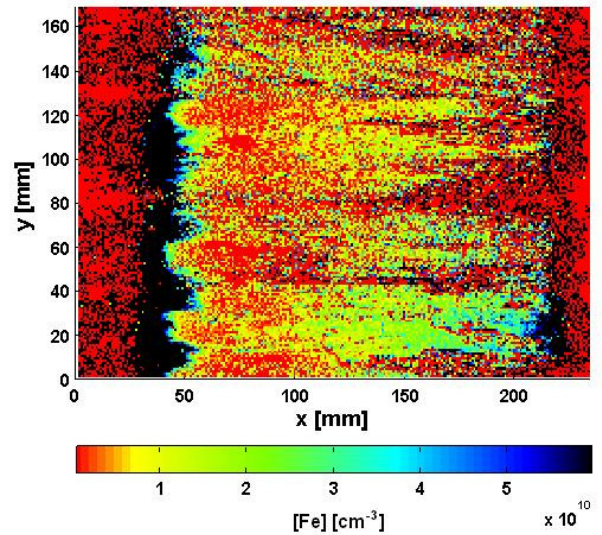
It is obvious that the measurement effect is about one decade higher for a steady state photogeneration. But below a Fe density of  $10^{10} \text{ cm}^{-3}$  the effect becomes even for steady state photogeneration very small (below 0.3  $\mu\text{s}$ ).

To determine the absolute iron concentration from the measured lifetime deviation, it is necessary to determine the correct injection and the correct calibration factor  $C$  in equation (3). This is achieved by determine the optical generation rate  $G_{opt}$  by using an effective width as proposed by Bowden et al. [10]. The injection can then be computed with:

$$\Delta n = \tau \cdot G_{opt} \quad (4)$$



a



b

**Figure 3** Minority carrier lifetime map and according relative iron concentration map of a typical mc-Si brick with a resolution of 1 mm

The correctness of the iron concentration determined by this procedure is still under investigation. Hence in the fol-

lowing the determined iron concentration is regarded as a relative concentration.

Regardless of the so far unknown accuracy of the iron determination, first measurement results indicate the value of this evaluation. Figure 3 displays a typical lifetime map and the according relative Fe density map with a resolution of 1 mm.

In figure 4 the average linescans versus the brick height are displayed. Figure 5 shows the average relative iron density versus the average lifetime of 5 typical bricks. From both figures it is obvious that the measured lifetime strongly depends on the iron concentration especially in the range between 5 and 35  $\mu\text{s}$ . Below a measured lifetime of approximately 5  $\mu\text{s}$ , no reliable iron detection was possible. Obviously in this case another recombination path is dominant, which disguises the iron effect, e.g. the recombination at crystalline defects. Above 35  $\mu\text{s}$  the detection limit for the iron density is reached. As predicted the detection limit lies in the range of  $10^{10} \text{ cm}^{-3}$ .

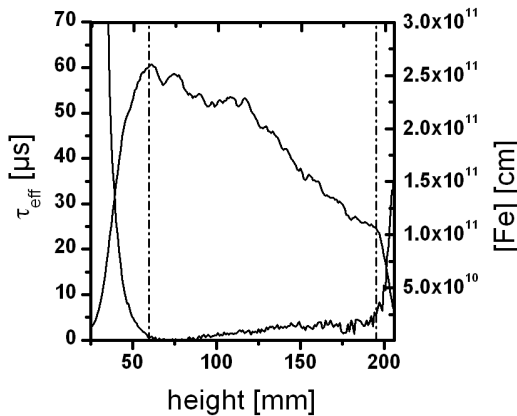


Figure 4 Average linescans of the minority carrier lifetime and relative iron density versus brick height

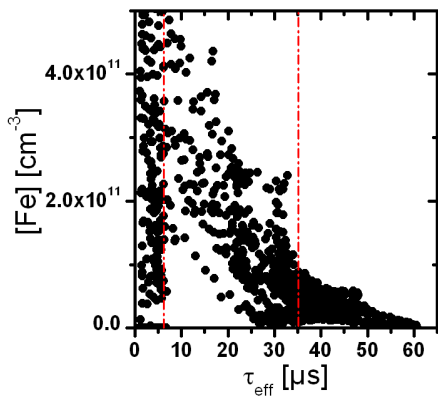


Figure 5 Relative iron density versus lifetime of 5 exemplary bricks

A first investigation of the iron density of bricks grown in two different crucible types showed a clear difference as expected from the given specification of these crucibles.

Also the average lifetime of these bricks deviated, ones more correlating with the iron density.

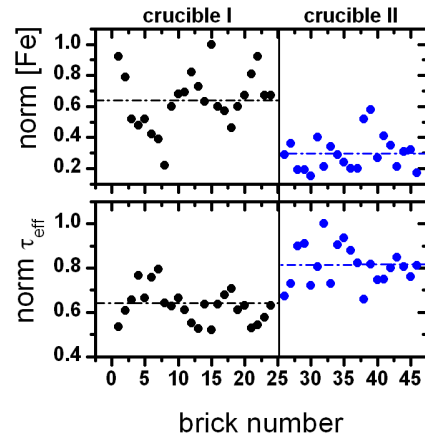


Figure 6 Relative iron density and minority carrier lifetime for a number of bricks grown in two different crucible types

These results confirm, that the minority carrier lifetime measured at as grown samples of solar grade material is first and foremost depending on the iron concentration and crystalline defects [11]. The effect of iron on the solar cell performance is comparatively low, since most of the iron is gettered or passivated during the phosphor diffusion and hydrogenation [12]. Hence an evaluation of the minority carrier lifetime and the iron density to separate the influences of iron and crystal defects, might improve the prediction of the solar cell performance.

### Pn junction detection

The PV industry currently strives to use more and more low quality material for low cost production of solar cells. Usually this low cost material as umg-Si contains a high phosphorus concentration, which can lead to a pn junction at the top of bricks. With the ability to measure the spatially resolved photoconductivity at as-grown bricks a new potential possibility of detecting pn-changes as early as possible arises. Hence more exact criteria for cutting off bad parts of the brick can be found.

A highly resolved resistivity measurement by eddy current measurements is very hard to achieve, so that in this case only a linescan in the middle of the brick is measured. The detection of a pn-junction with only one resistivity linescan is very inaccurate, because the junctions often proceed diagonal or with a strong bow through the brick. With the highly resolved photoconductivity map, these problems can be overcome.

The measured photoconductivity or signal height strongly depends on the resistivity, which rises sharply at a pn-junction. With a clever computer algorithm the sharp rise of the photoconductivity can be detected with a resolution of 1 mm.

In figure 6 a photoconductivity map of a mc-Si brick with a pn junction is depicted. The pn-junction at a height of ap-

proximately 250 mm can be easily recognized, because of the much higher photoconductivity.

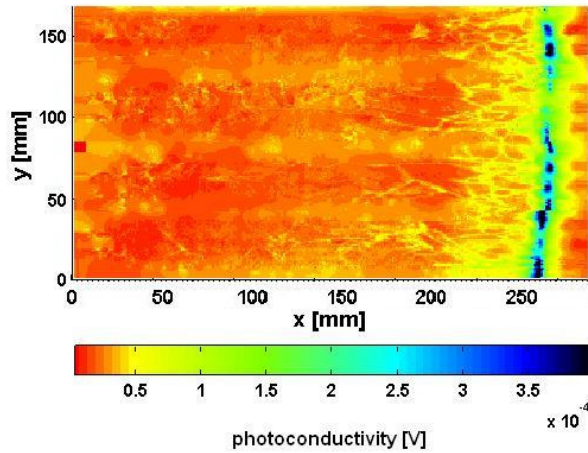


**Figure 6 Photoconductivity map of a mc-Si brick with a pn junction**

In figure 7 the average linescan of the photoconductivity and the linescan of the resistivity versus the brick height are displayed. The sharp rise in both parameters is very obvious, but at slightly different positions, because of the problems at resistivity measurements mentioned above.

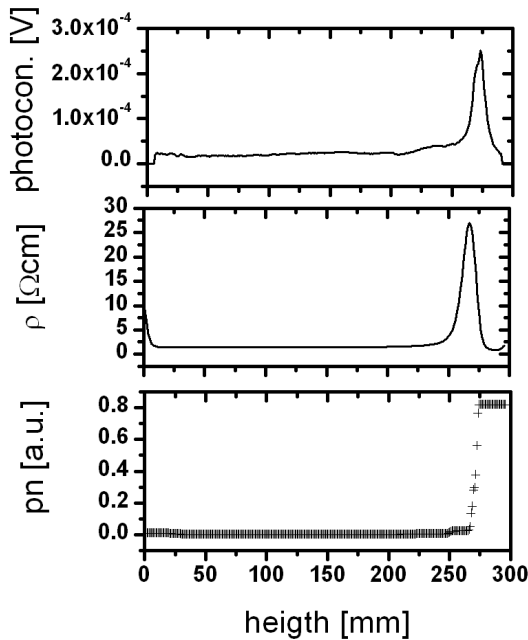


**Figure 7 The according average linescan of the photoconductivity and resistivity plus the output of the detecting computer algorithm versus brick height**

In figure 7 the output of the pn detecting algorithm is also depicted and indicates that the algorithm is working correctly.

**Correlation with efficiency and open circuit voltage**

As mentioned before the correlation between the minority carrier lifetime of as grown bricks and the open circuit voltage or efficiency of the resulting solar cells is not very good. The reason for that seems to be the influence of iron. To overcome this problem different parameters were investigated for a statistical number of bricks.

Besides iron, crystal defects have a huge influence on the minority carrier lifetime and there influence is not changed so dramatically by the processing steps. As shown above especially the very small measured lifetimes (under 10  $\mu$ s) seem to be due to crystal defects. Hence the correlation between the quantile of 10  $\mu$ s (that means the percentage of measured lifetimes below 10  $\mu$ s) versus the brick height with the open circuit voltage was investigated. Figure 8 shows the result for two exemplary bricks. Especially in the good part of the brick, the correlation is very good. Obviously in the bottom and top of the bricks other defects influence the open circuit voltage.

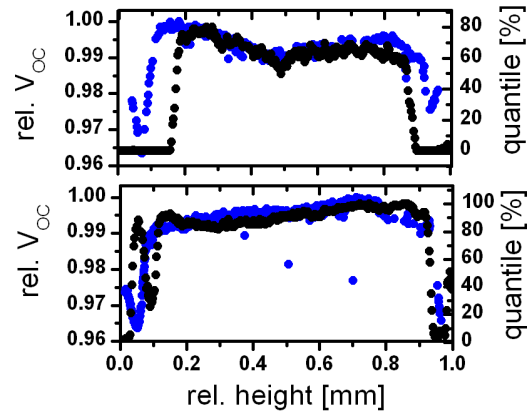


**figure 8 Relative open circuit voltage and quantile versus relative brick height for two bricks**

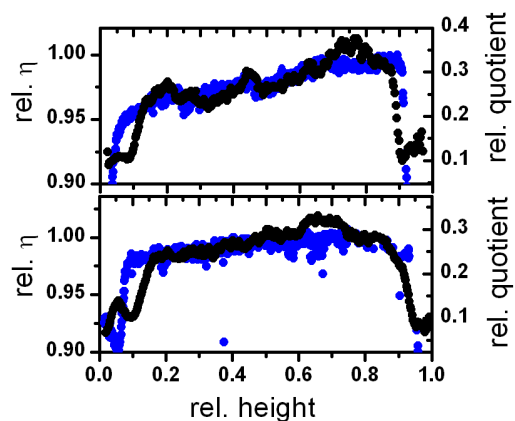


**Figure 9 Relative efficiency and relative quotient of lifetime and photoconductivity versus relative brick height for two exemplary bricks**

## 35th IEEE Photovoltaic Specialists conference, Honolulu Hawaii

Another interesting parameter is the quotient of minority carrier lifetime and photoconductivity at steady state. Since the photoconductivity also depends on the mobility and rises if traps are present, this quotient gives important information about defects in the brick. As can be seen in figure 9, the relative quotient correlates well with the cell efficiency.

The results of such correlation studies may be different for different solar cell producers. The comprehensive software supplied with every MDP tool enables to investigate these correlations for a vast amount of samples in a short time.

### CONCLUSION

To summarize, MDP is a method well suited for inline measurements. Especially the high spatial resolution, the very short measurement time and the simultaneous measurement of two sides of a brick make MDP predestined for inline metrology. Because of its outstanding qualities MDP enables advanced process control and yield relevant parameter optimizations.

Simulations and measurements proved that the measured effective lifetime is only lightly influenced by the surface and that the determination of the iron density is enabled. Furthermore it could be shown, that a detection of p-n junctions in the bricks is possible. All these features along with the comprehensive software supplied with the measurement tool enable a variety of applications and facilitate the detection of errors in the growth process, detrimental impurities in the feedstock or the optimization of furnace parameters.

### ACKNOWLEDGEMENT

This work was supported by the European funds for regional Development (EFRE) 2007-2013 and the state Saxony.

### REFERENCES

- [1] K. Dornich, T. Hahn, and J.R. Niklas, "Non destructive electrical defect characterization and topography of silicon wafers and epitaxial layers", *Material Research Symposium Proceedings* **864**, 2005, pp. 549-554.
- [2] K. Dornich et al., "Contact Less Investigation of Electrical Properties and Defect Spectroscopy of mc-Silicon at Low Injection Levels", *DRIP XI*, 2005, Peking (China).
- [3] K. Dornich et al., " New Spatial resolved inline metrology on multicrystalline silicon for PV", *24th PVSEC*, 2009, Hamburg (Germany).
- [4] S. Hahn et al., "Contact-less Electrical Defect Characterization of Semi-insulating 6H-SiC Bulk Material", *Materials Science Forum* **600-603**, 2009, pp. 405-408.
- [5] D. Klein, F. Wuensch, and M. Kunst, "The determination of charge-carrier lifetime in silicon", *Physica Status Solidi B-Basic Solid State Physics* **245**, 2008, pp. 1865-1876.
- [6] R. Sinton, A. Cuevas, and M. Stuckings, *Proceedings of the 25th IEEE PVSC*, 1996, pp. 457-460.
- [7] S. Rein, and S.W. Glunz, "Electronic properties of interstitial iron and iron-boron pairs determined by means of advanced lifetime spectroscopy", *Journal of Applied Physics* **98**, 2005, 113711.
- [8] T. Hahn, "Numerische Modellierung und Quantitative Analyse der Mikrowellendetektierten Photoleitfähigkeit (MDP)", *Experimentelle Physik*, 2009, TU Bergakademie Freiberg.
- [9] N. Schüler, et al., "Theoretical and experimental comparison of contact less lifetime measurement methods at thick silicon samples", *Solar Energy Materials and Solar Cells* **94**, 2010, pp. 1076-1080.
- [10] S. Bowden, and R.A. Sinton, "Determining lifetime in silicon blocks and wafers with accurate expressions for carrier density", *Journal of Applied Physics* **102**, 2007, 124501.
- [11] G. Coletti et al., "Effect of iron in silicon feedstock on p- and n-type multicrystalline silicon solar cells", *Journal of Applied Physics* **104**, 2008, 104913.
- [12] S. Dubois et al., "Effect of intentional bulk contamination with iron on multicrystalline silicon solar cell properties", *Journal of Applied Physics* **102**, 2007, 083525.